705

Fermilab Proposal No. ~~669~~
Scientific Spokesman:

Brad Cox
Fermilab

FTS No: 312-370-3152
Commercial No:
312-840-3152

P669

REVISED OBJECTIVES

(September,1981)

A Study of Charmonium and Direct Photon Production by 300GeV/c Antiproton, Proton, π^+ and π^- Beams

M. Binkley, B. Cox, K. K. Gan, C. Hojvat, D. Judd, R. Kephart, P. Mazur, C. T. Murphy, F. Turkot, R. Wagner, D. Wagoner, W. Yang

Fermi National Accelerator Laboratory

E. Anassontzis, P. Karabarbounis, S. Katsanevas, P. Kostarakis, C. Kourkoumelis, P. Ioannou, A. Markou, L. Resvanis, C. Trunalinnos, G. Voulgaris

University of Athens

H. Areti, S. Conetti, P. Lebrun, D. Ryan, T. Ryan, W. Schappert, D. Stairs

McGill University

He Mao, Zhang Nai-jian

Shandong University
Peoples Republic of China

ABSTRACT

The large aperture spectrometer of E-537 and the special high intensity secondary beams which are available in the High Intensity Laboratory of the Proton Area in the Tevatron era offer a unique opportunity to study the hadronic production of χ states and their subsequent decays and the production of direct photons. We are revising our priorities and apparatus as outlined in our previous P669 and E-537 proposal submissions [1] to emphasize good energy resolution of the final state photons with the primary intention of studying the hadronic production of χ states by proton, antiproton, and $\pi^{\pm}$ beams.

$$\left(\frac{p^{\pm}}{\pi^{\pm}}\right) + N \rightarrow \chi + X$$

A 1500 hour experiment at 300GeV/c using the E-537 apparatus augmented by the proposed high resolution electromagnetic shower detector (See Appendix A) will allow us to accumulate a data sample of greater than 10^5 χ decaying $\rightarrow \gamma\psi$. The good energy resolution of the spectrometer for both charged particles and photons will allow us to resolve the 1^{++} and 2^{++} charmonium states. With the good acceptance afforded us by our large aperture spectrometer we will be able to study χ production in the region $.0<x_F<.8$ and at $P_\perp$'s up to 4GeV/c and χ decay into $\gamma\psi$ over the entire range of the decay angles. Such measurements should provide an understanding of the various mechanisms (quark

and gluon fusion) involved in the production heavy quark bound states.

Simultaneously with the charmonium photons we will measure the high $P_\perp$ and high x_F production of direct photons by the same beams.

$$\begin{pmatrix} p^\pm \\ \pi^\pm \end{pmatrix} + N \rightarrow \gamma + X$$

The direct photon data collected during this run will allow a unique measurement of the difference of proton and antiproton production of direct photons out to $P_\perp \sim 8$ GeV/c and over the entire range of $x_F > 0$. At the same time in the same apparatus we will measure $\pi^\pm$ production of direct photons and be able to compare these measurements to the antiproton measurement. The antiproton-proton comparison should allow the separation of the quark-antiquark annihilation and gluon-quark components of direct photon production and allow the continuation of the study of valence quark and gluon structure functions (begun in E-537 with the study of lepton pair production by antiprotons) to regions of much higher x_F and $P_\perp$.

II Physics Goals

A. Charmonium Production in Hadronic Interactions

The high resolution E-537 spectrometer (See Figure 1) and its associated di-muon trigger processor [2] will be augmented by the high resolution electromagnetic shower detector described in Appendix A. This system together with the unique mixture of high intensity antiproton, proton, $\pi\pm$ beams available in the High Intensity Laboratory of the Proton Area will enable us to study, as a first priority, the production of charmonium χ states which decay into $\gamma\psi$. With the excellent mass resolution of our spectrometer we will be able to resolve the 2^3P_J states and with high statistics to study their production and decay angular distributions in various kinematic regions. The comparison of the hadronic production of the various χ states by antiprotons, protons, and $\pi\pm$ will allow us to test the predictions of the various gluon and quark fusion models[3-13] and to eventually extract the gluon structure functions. In particular the study of the difference of $\bar{p}N$ and pN production of the various χ states will allow the isolation of the contribution due to the nuclear valence quarks. Furthermore, for all incident beams a detailed study of the decay angular distributions of the individual χ states can help determine the production mechanisms[12-13]. Also, a determination of the cross section for the various χ states vs x_F and $P_\perp$ will be an additional stringent test of the various ideas for the production of these states by constituent interactions. Finally with the addition of the Cerenkov counters C1, 2, 3 (See

Appendix B), the high statistical levels and the good mass resolutions for the χ and ψ states will allow us to continue the search[58] for the expected decays[59] of beauty, $B \to \psi K$ and $B \to \psi K\pi$. In addition, we will be able for the first time to search for the similar decays $B \to K\chi$ and $B \to \chi K\pi$.

B. Direct Photon Production in Hadronic Interactions

While performing the measurement of χ production and decay we will accumulate a large amount of high $P_\perp$ and high x_F direct photon data produced by the antiproton, proton, and $\pi^\pm$ beams. This data (especially the unique capability of doing a proton - antiproton difference) would add greatly to the observations of direct photon production at high $P_\perp$ in proton-nuclear interactions which have been performed at Fermilab and at CERN[14-17]. This process is thought [18-22] to proceed in lowest order in α_s via the interactions of the constituent quarks and gluons shown in the following diagrams:

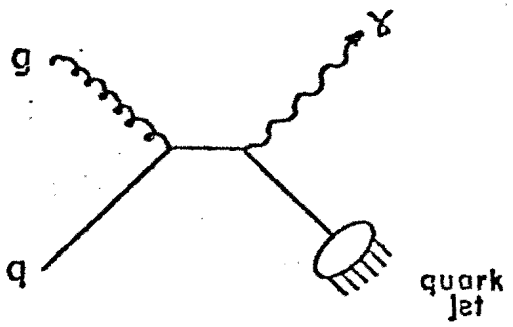

COMPTON

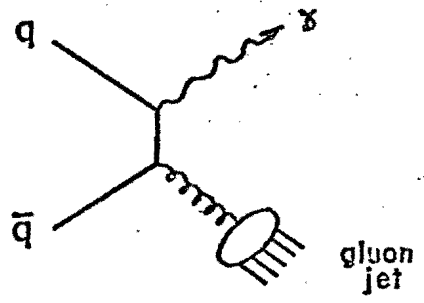

ANNIHILATION

As shown above, the production of direct photons by protons or π^+ in this picture will be dominated by the Compton process since the annihilation process proceeds mainly via valence antiquarks. The antiproton and π^- interactions will have approximately equal contributions from the two diagrams at moderate $P_\perp$ but at higher $P_\perp$ the annihilation process will dominate. By measuring the difference of the antiproton and proton cross sections from our isoscalar D_2 target we will isolate the annihilation process and be able to study the nucleon valence quark structure functions at high $P_\perp$ and x_F. The same statement is true for for the $\pi^- D_2$ and $\pi^+ D_2$ difference except in this case the pion valence quark structure functions are studied.

In summary while accumulating the χ data we will collect a major amount of high $x_\perp$ and x_F direct photon data which will allow us to accomplish the following studies:

1.	$\sigma_\gamma(\bar{p}D) - \sigma_\gamma(pD)$	study of the annihilation process for nucleon valence quarks, for higher statistics extraction of the nucleon structure functions, at high x_F and $P_\perp$.
	$\sigma_\gamma(\pi^- D) - \sigma_\gamma(\pi^+ D)$	Study of the annihilation process for pion valence quarks at large X_F and $P_\perp$.
2.	σ_γ (pD)	study of the Compton process, and study of the nucleon glue distribution.
	$\sigma_\gamma(\pi^+ D)$	study of the Compton process and study of the pion glue distribution. This process is complicated by a 25% admixture of the annihilation process.
3.	$\sigma_\gamma(\bar{p}D)$	comparison of the antiproton production of direct photons themselves with the antiproton production of dimuons (which is being measured in E-537) by comparison of the extracted structure functions.

II Beams

We will split the requested 1500 hours for this experiment equally between positive and negative beam running. The beam energy is chosen to be 300 GeV/c for this phase of the experiment since this is the energy at which an adequate flux of identifiable antiproton (and π^+) are available for the antiproton-proton (and $\pi^\pm$) comparison aspects of the experiment (See Table I). We have taken as a limitation either the available protons for the High Intensity Laboratory from the Doubler (2.5×10^{12} protons/spill) or a maximum secondary beam flux which can be handled either by our beam tagging system or the E-537 spectrometer in the open geometry configuration shown in Figure 1. These beams correspond to a maximum interaction rate of 2.5×10^6 interactions/sec in our 1 meter D_2 target. Deuterium is chosen both for its I=0 nature and in order to optimize the ratio of radiation length to interaction length in the target material.

We show in Figure 2 the positive and negative secondary beam yields[23] available with the 1000 GeV/c Tevatron. We will use both the unique $\bar{\Lambda}^\circ \to \bar{p}$ beam[24] (hereafter referred to as the neutral beam) for the negative beam operation and the conventional secondary transport[25] (referred to as the charged beam) for the positive beam running. The existing beam tagging system utilizes two 70' long differential Cerenkov counters operating at $\theta_c \sim 6.5$ mrad. They work well up to a beam momentum of 150 GeV/c. At 300 GeV/c we would employ two 95' long threshold Cerenkov counters

(θ_c=3.1 mrad with an average of four photoelectrons per counter). With the particle ratios shown in Table I, these Cerenkov counters will allow less than 1% π^- contamination of the antiproton flux.

Table I

Beam Scenario

Primary Proton Beam Energy	- 1000 GeV/c
Secondary Beam Energy	- 300 GeV/c
Spills/hour	- 100
Spill Length	- 10 Seconds
Length of Run	- 750 hours - Neutral Beam ($\bar{\Lambda}^0 \rightarrow \bar{p}$) for $\pi^-/\bar{p}$ 750 hours - Charged Beam for π^+/p
Protons/spill	- 2.5×10^{12} for Neutral Beam operation ~ 10^{10} for Charged Beam operation
Secondary Beam/spill	- 4.0×10^7 π^- - 0.8×10^7 $\bar{p}$ for Neutral Beam operation
	- 4.0×10^7 p_+ - 6.0×10^7 π^+ for Charged Beam operation
Interaction Rate (1 meter D_2 target)	- 1.1×10^6 int/sec for Neutral Beam operation
	- 2.5×10^6 int/sec for Charged Beam operation
Total Beam	- 5.5×10^{11} $\bar{p}$ 2.8×10^{12} π^- for 750 hours of operation
	3.0×10^{12} p_+ 4.5×10^{12} π^+ for 750 hours of operation

III Apparatus

The apparatus to be used in this experiment (See Figure 1) is basically the E-537 spectrometer augmented by a high resolution electromagnetic shower counter array (See Appendix A) for photon measurement and a set of segmented Cerenkov counters for charged particle identification. These devices are described in Appendices A and B of this proposal. The electromagnetic shower counter array was chosen to be Pb glass because of the good photon energy resolution. This energy resolution will allow a good χ mass resolution and a comfortable separation of the 1^{++} and 2^{++} χ states in all kinematic regions of χ production and decay. The general parameters of the spectrometer are given in Table II below:

Table II

Vertical Aperture	±100 mrad
Horizontal Aperture	±200 mrad
$\int B.d\ell$	1089 kG inches

Resolutions (σ):

Mass ψ (3 GeV/c^2)	40 MeV/c^2
Mass T (10GeV/c^2)	190 MeV/c^2
*Mass χ_ψ(3.5 GeV/c^2)	11 MeV/c^2 (8 MeV/c^2)**
*Mass χ_T(10.0 GeV/c^2)	17 MeV/c^2 (11 MeV/c^2)**
E resolution for γ	$\frac{\sigma}{E} \sim \frac{4.3\%}{\sqrt{E}} + 0.7\%$ $\left(\frac{\sigma}{E} \sim \frac{2.0\%}{\sqrt{E}}\right)$**
P resolution for charged particles	$\sigma \sim 0.2\% . \sqrt{p^2 + Q.01p^4}$
Position resolution - Electromagnetic shower counter array	$\sigma_x \sim 11mm/\sqrt{E}$
Position resolution - Drift Chamber	$\sigma_x \sim$ 200 microns
π^0 Mass resolution	$\sigma/m \sim$ 6.5%
η^0 Mass resolution	$\sigma/m \sim$ 3.0%
Resolving distance for two photons	~ 2 inches

*Requires constraint of ψ(T) mass

**We quote two numbers for χ resolution for two different compositions of the electromatnetic shower counter array. The first number is that expected for an array constructed entirely from SF5 Pb glass. The energy resolution given in Table II is based on the experiences of the Mark II Pb glass wall and E-238. The resolutions given in parenthesis are those expected for an array composed of a mixture of Ohara scintillator glass SCG1-C and SF5 (See Appendix A).

IV Measurement of χ Production by $p^{\pm}$ and $\pi^{\pm}$ Beams

A. Event Rates

To estimate the number of χ's which we will accumulate in our 1500 hour, 300 GeV/c experiment we have used the measured cross sections[26-29] for ψ (3.1) production for π^- and proton beams and the experimentally observed ratios

$$\frac{\sigma(\bar{p}N \rightarrow \psi + X)}{\sigma(pN \rightarrow \psi + X)} = 1.4 \qquad \frac{\sigma(\pi^- N \rightarrow \psi + X)}{\sigma(\pi^+ N \rightarrow \psi + X)} = 1.0$$

In addition, we have made the assumption in calculating the acceptances of our spectrometer and the yields of χ's at various x_F and $P_\perp$ that the χ production (as a function of x_F and $P_\perp$) looks very much like ψ production.

Using these data and assumptions we can estimate the level of χ production by using the various measurements[30-32] of the ratio of χ hadroproduction to ψ hadroproduction. We have taken the observations of reference[32] for $\pi^- N \rightarrow \chi X$ at 175 GeV/c as the most current and appropriate to our experiment. Using their result

$$\frac{\pi^- N \rightarrow \chi X}{\pi^- N \rightarrow \psi X} = .36 \pm .05$$

we have predicted the number of χ's which should be produced by each beam. Since the relative hadroproduction cross sections for the various χ states are unknown we have assumed for the preparation of Figure 3 and Table III that the 2^3P_J states have equal production cross sections (in contradiction to the prediction of the gluon fusion model[3]). The $2P_1$ state has been

ignored since it has not been observed in e^+e^- reactions. However it is possible that this state could be observed in a hadronic experiment since its production in e^+e^- experiments must proceed via the production of a ψ' with the subsequent decay of the $\psi' \to \gamma\chi \to \gamma\gamma\psi$. This chain may be suppressed because of a small $\psi' \to \gamma\chi$ branching ratio. The branching ratios of $\chi \to \gamma\psi$ used in the preparation of Table III and Figure 4a,b have been taken from reference[33].

TABLE III

Number of Observed $\psi \to \mu^+\mu^-$ and $\chi \to \gamma\psi$ Events

Beam \ Resonance	ψ	χ States 0^{--}	1^{++}	2^{++}	Total χ's
$\bar{p}$	38K	.6K	7K	3.4K	11K
π^-	134K	2.6K	30K	14.6K	47K
P	150K	2.3K	27K	13.0K	42K
π^+	214K	4.1K	48K	23.3K	75K
Mass→	3. 10GeV/c^2	3.415 GeV/c^2	3.510 GeV/c^2	3.550 GeV/c^2	-

Number of χ's vs. X_F

X_F \ Beam	$\bar{p}$	π^-	P	π^+
<-.2	70	100	250	160
-.2 to .0	2150	3450	5700	5600
.0 to .2	5550	19000	23500	30600
.2 to .4	2700	18000	10150	29000
.4 to .6	500	5150	2200	8300
>.6	40	850	150	1400

Number of χ's vs. $P_\perp$

$P_\perp$ \ Beam	$\bar{p}$	π^-	P	π^+
0-1	6200	26500	23500	43000
1-2	4400	18300	16600	30000
2-3	850	1700	1600	2700
3-4	-	25	-	40

B. Backgrounds

We have estimated the combinatorial background to χ states that arises when an event containing a $\psi(3.1)$ also contains one or more photons from a π^0 or η decay in which the other decay photon is missed. Typical events with π^0's and η's have been generated from $\bar{p}p$ bubble chamber[34] events and ψ production has been superimposed on them. All final state photons which can be combined to reconstruct an η or a π^0 have been eliminated from the $\gamma\psi$ combinations which make up the background. The remaining $\gamma\psi$ events properly normalized make up the backgrounds to the 2^3P_J spectrum shown in Figures 3a and b.

C. Resolutions

The mass resolution which we expect to achieve for the χ spectrum is given in Table II and exhibited in Figures 3 and 4. As stated in Table II the resolution depends on the ultimate composition of the electromagnetic shower counter array. We have estimated the resolution for an array that is composed entirely of SF5 Pb glass. We plan, however, to construct the central part of the array (See Appendix A) out of the new scintillator glass, SCG1-C from Ohara Optical. The better energy resolution which has been measured for this glass as well as its measured two order of magnitude increase in resistance to radiation yellowing results in the more comfortable χ mass resolution shown in Figure 3a and a more stable detector. With either glass type we expect to be able to resolve the 1^{++} and 2^{++} χ states but with the high

resolution glass the sensitivity of the measurement will be increased, the range of x_F and decay angles of the X states over which the 1^{++} and 2^{++} are well resolved will increase, and the background contamination of the angular distibutions will be reduced.

D. Acceptances

As indicated in Section IV A the acceptances for χ events are quite good (averaged .28 for p± induced events and .35 for π± induced events at 300GeV/c over all x_F and $P_\perp$). However, it is important to have good acceptance in the χ decay angles which must be measured in order to isolate the production mechanisms. According to various theoretical predictions[12-13] the angle between the photon and the beam (θ) and the angle between the photon and the positive lepton (β) in the χ center of the mass are important in separating gluon and quark production mechanisms. We show the acceptances vs $\cos\theta$ and $\cos\beta$ in Figure 5. Note that the acceptance in $\cos\beta$ is almost flat. The acceptance of our experiement at negative $\cos\theta$ is quite good because of the ability of our shower array to detect low energy and wide angle photons. (We apply a 300 MeV energy limit on observable photons even though the noise level in our glass shower counters is expected to be less than 100 MeV from our previous experience). We see positive $\cos\theta$ in a relatively unbiased way except for a small region near $\cos\theta=1$. where the χ decay photon is lost in the beam hole.

E. Trigger Rates

The trigger with which we plan to accumulate our resonance data is basically the same di-muon fast trigger which has already operated in E-537. We expect to use our existing trigger processor[2] to impose a di-muon mass cut to eliminate triggers from low mass muon pairs. In an open geometry configuration of E-537 the major contribution to the trigger rate will be two decaying pions producing a di-muon trigger. We have estimated from bubble chamber data and a software simulation of our fast trigger and trigger processor the trigger rates which are given below for the expected interaction rate for the 300GeV/c positive and negative beam operation.

Beams	Fast Logic Triggers per sec	Di Muon Triggers/sec 2 GeV Trigger Processor Cut
$\bar{p}/\pi^-$	1300	$\sim$ 60
p/π^+	2900	$\sim$125

As can be observed the rate which the trigger processor is required to handle is quite reasonable and the number which pass the trigger processor cut can be handled by the online data acquisition system.

V. Measurement of Direct Photon Production by p± and π± beams

A. Event Rates

Direct photon production in proton-nucleon interactions has been observed by several experiments both at Fermilab[14] and CERN[15-17]. The currently existing data is shown as a function of

$P_\perp$ in Figure 6. Attempts have been made by a number of theorists[18-22] to calculate the production of direct photons within the framework of QCD. These efforts have resulted in a consistent picture of direct photon production. In particular, the theoretical curves of Figure 6 represent the results of a calculation[19] which approximately fits all existing data. The sensitivity of the calculation to the choice of the intrinsic transverse momentum spectrum of the constituents is indicated by the $K_T = 0$ and 1 GeV/c dashed and solid curves.

Since no published data exists at the present time for direct photon production by $\pi^\pm$ and no data at all for $\bar{p}$ we have estimated the expected cross sections for these reactions from a QCD calculation similar to that which fits the proton-nucleon direct photon production. The Compton and annihilation processes have been calculated and summed using the usual formalism[35]:

$$\frac{d^2\sigma}{dp_\perp{}^2 dy} = \left[s \int_{X_{1_{min}}} \left(\frac{d\sigma}{dt'}\right)_C \left(\frac{1}{X_1 s+u}\right) \left(\sum e_q^2 \;\; G.F + \text{beam}\leftrightarrow\text{target}\right) \; dX_1 \right.$$

$$\left. + s \int_{X_{1_{min}}} \left(\frac{d\sigma}{dt'}\right)_A \left(\frac{1}{X_1 s+u}\right) \left(\sum e_q^2 \; F.F + \text{beam}\leftrightarrow\text{target}\right) \; dX_1 \right]$$

where: the $\frac{d\sigma}{dt'}$ are the appropriate subprocess cross sections for

the Compton and annihilation diagrams, G and F are the gluon and quark structure functions with Q^2 dependence for the appropriate hadrons, s and u are the usual Mandelstam variables for the interaction, and t' is the momentum transfer in the constituent subprocess. We have used the structure functions tabulated in references[36] and [37] with the gluon structure function modified to the strong glue form[38]. The intrinsic transverse momentum distribution of the gluons and partons is introduced via the Altarelli-Parisi method[39, 40]. The average intrinsic transverse momentum is chosen to be 600 MeV/c to agree with that extracted from the μ pair production data of references 41, 42 and 43.

In Figures 7a,b and 8a,b we show the direct photon cross sections which we expect for $p^{\pm}$ and $\pi^{\pm}$ interactions at 300 GeV/c as a functions of $p_\perp$ and x_F in order to demonstrate several interesting features. It appears that at high $p_\perp$ the annihilation process is larger than the Compton process in the production of direct photons. This dominance of the annihilation process as shown in Figure 7a,b is true regardless of whether strong or weak glue structure functions are present. In addition, as shown in Figure 7a,b, the annihilation process is much larger in π^- and $\bar{p}$ induced reactions than in the π^+ or p interactions because of the presence of valence antiquarks of charge 2/3. These features lead to the expectation that the hadrons recoiling against the high $p_\perp$ direct photon will more often be the result of gluon fragmentation than quark fragmentation.

When an isocalar target such as deuterium is employed, the difference of the $\bar{p}$ and p or the π^- and π^+ induced direct photon signals should be the contribution due to the annihilation process and should contain indications of gluon jets. In addition the difference between the π^+ and π^- cross sections should be free of residual backgrounds to the direct photon production which are due to photons from π^0 and η decay since π^0 and η production should be the same for π^+ and π^- interactions with D_2 by isospin arguments. The same background statement should be approximately true for $\bar{p}/p$ differences, although in this case an isospin argument cannot be made. In addition the $pD \to \gamma X$ and to a lesser extent, the $\pi^+ D \to \gamma X$ reactions are dominated by the Compton process. Therefore, by examining these reactions it is possible to study an almost pure Compton process and to search for evidence of quark jets. However, in this case the direct photon backgrounds must be estimated from the observed π^0 and η production and taken into account.

Using the above QCD calculation, direct photon event rates for each of the 300 GeV/c beams have been calculated and are given in Figures 8, 9 as a function of $p_\perp$ and x_F. The large numbers of direct photons which are produced for each type of beam particle are adequate to probe the large x_F and $p_\perp$ in which QCD may be valid.

B. Backgrounds to Direct Photons

Unlike the production of dileptons (which is suppressed by a factor of α relative to direct photons at a given x_F and $p_\perp$), the problem with direct photons is not one of event rate, but rather one of backgrounds. Both by the technique of taking differences of cross sections and by eliminating π^0 and η photons we will achieve clean direct photon signals.

The major backgrounds for the direct photon part of the experiment arise from several sources:

1. Single photons from π^0, η (ω^0,η',χ, etc.) decay are lost outside the electromagnetic shower detector or in the 6" x 6" beam hole. Approximately 85% of the total background is due to loss of photons at large angles.

2. Asymmetric π^0, η decay in which one of the photons from the π^0 or η is so low in energy that it is not recognizable in the the neutral detector. This is less than 1% with our 300 MeV cutoff in energy. Our previous experience with Pb glass indicates that a 100 MeV cutoff is probably possible.

3. Events in which one photon from a π^0 decay converts in the deuterium target or in another part of the spectrometer and the e^+e^- pair is not recognized as such in the spectrometer. This source contributes less than 2% of the total background.

4. Coalescing photons from π^0 decay or overlap of photons from the decay of different π^0's. The coalescing leads to approximately 6% of our total backgrounds if a conservative 2" is required between photons in this shower detector in order to consider them distinguishable. The overlap of different π^0 photons leads to another 6% of the total background.

5. Neutral hadrons. By examining the longitudinal and transverse sharing of the shower by the various counters composing the live converter and the main body of the shower array we estimate (using our previous experience[14] and the experience of other experiments[15,16], a background from this source that is less than 1% of the final signal level.

We have simulated backgrounds 1-4 in order to arrive at these estimates by using measured π^0 and η fluxes[44,45] to make a monte carlo calculation of the photon flux expected in the spectrometer. For the case of $\bar{p}p \to \pi^0 X$ we have assumed that the cross section is approximately the same as that of $pp \to \pi^0 X$. We use the scaling form

$$E\frac{d^3\sigma}{dp^3} = A\ p_\perp^{-N}(1-X_R)^M \qquad X_R = \sqrt{X_\perp^2 + X_F^2}$$

with N=9, M=5, and A = 3.8 x 10^{-27}cm^2/GeV^2/nucleon. This form fits the data of reference 44 for pN interactions. The $\pi^\pm p \to \pi^0 X$ cross sections are taken from reference 45:

$$E\frac{d^3\sigma}{dp^3} = A'\ (1 - X_D)^F/(p_\perp^2 + 0.97)^N \qquad X_D = \sqrt{X_\perp^2 + (X_F - 0.14)^2}$$

with N=5, F=3, and A'=1.1 x 10^{-26}cm^2/GeV^2/nucleon. An η/π^0 ratio of 0.5 measured in these two experiments[44, 45] is used in simulating the background due to η. The production of ω^0, η', χ has been measured[46] and the backgrounds they cause are estimated to be insignificant. Using these cross sections we have simulated the π^0 and η production and investigated the properties of the spectrometer. We have eliminated background photons in our simulation by computing the invariant mass of all two photon combinations and reconstructing π^0's and η's. All residual photons which are unpaired for any of the reasons 1-4 are direct photon candidates and form the majority of the background. Clearly, the energy and position resolution of the detector are important in providing positive identification of a two-photon

pair as a π^0 or an η. The properties of the detector described in Appendix A are such that the mass resolutions at 300 GeV/c are $\sigma_{\pi^0} \sim 8 MeV/c^2$ and $\sigma_\eta \sim 15 MeV/c^2$.

In Figs 9,10 we show our estimates of the remaining residual background vs $p_\perp$ and x_F. The signal to background improves both at high $p_\perp$ and x_F. For the high $p_\perp$ and x_F regions where the signal/background ratio is large, the direct photon flux will provide a clean signal for extraction of structure functions.

C. Trigger Rates for Direct Photons

We plan to construct a high $p_\perp$ trigger for our electromagnetic shower detector by grouping the 426 counters of the shower detector into sets of 9 counters which form square "trigger regions". The signals from each individual counter are fanned out (by 9) and are resummed (again by 9) to form an energy for each trigger region. To form the $p_\perp$ trigger these signals are required (by simple setting of discriminator levels) to be above a threshold which depends on the distance of the center of the trigger region from the beam. We have estimated with our monte carlos for this very simple regional $P_\perp$ trigger the rates for each beam above $P_\perp$ pf 4.0 GeV/c.

300GeV/c Beam	Trigger Rate/sec
$\bar{p}/\pi^-$	$\sim$ 10
p/π^+	$\sim$ 25

Thus the total trigger rate including real direct photons and background photons is quite manageable.

APPENDIX A

P669 Electromagnetic Shower Detector

We have chosen to aim for the best possible photon energy resolution in our neutral detector in order to make the χ mass resolution as comfortable as possible. This criterion implies a glass shower detector. We intend to add the electromagnetic shower counter array shown below to the E-537 spectrometer in order to accomplish the goals of the proposal.

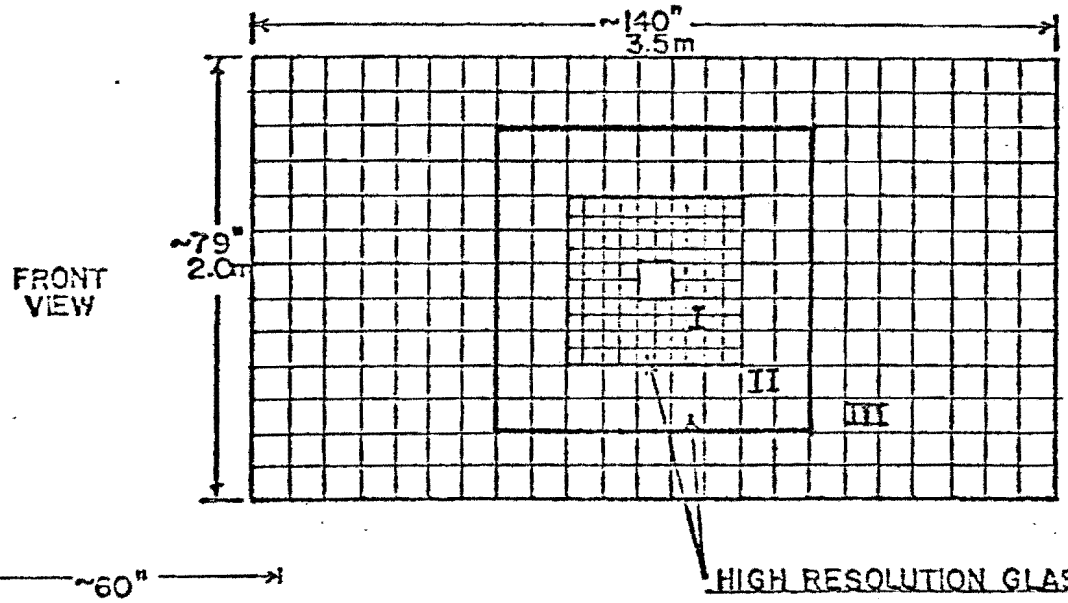

HIGH RESOLUTION GLASS SECTIONS I,II

(Preferably SCG1 glass in Regions I, I
SF5 glass adequate for Region III

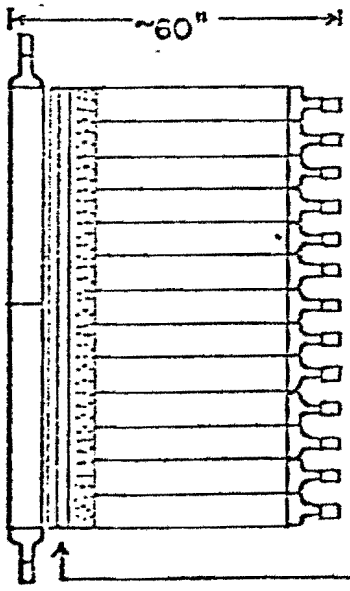

Counter Composition of EM Detector

1. Live Converter- size (6"x6"x39")* - 46 counte
2. Main Body I - size (3"x3"x34")* - 96 "
3. Main Body II - size (6"x6"x34")* - 56 ... "
4. Main Body III - size (6"x6"x]6") - 228 "

Totals 426 counte

*Assumes SCG1-C scintillator glass is used. Lengths would be different for Main Body I & II if SF5 is used.

6 Planes PWC (2MM spacing ganged together in 1c strips, 3X planes, 3Y planes)
1cm polyethylene separating planes
1650 channels total

As indicated the shower detector array consists of 426 individual glass counters in the arrangement of a live converter followed by a 6 plane PWC station with 2mm wire spacing followed by the main body of the shower counter. The PWC station has its signal wires ganged together to form 1cm strips, each of which is digitized to provide precision spatial information about the photon position in the detector. Previous experience of other experiments indicates that a position resolution of $\sigma \sim 2$mm can be achieved with this strip width for photon energies of 30 GeV. For lower energy photons we have used $1/\sqrt{E}$ dependence, a conservative assumption which has been bettered in various experiments. The 6 signal planes of the PWC station are separated by approximately 1cm of polyethylene in order to range out low energy electrons.

We have considered two possible types of glass for the shower counters which compose the detector. SF5 is a standard Pb glass that has been widely used in the past and would be adequate for this detector. However, it has an energy resolution which is ultimately limited by photon statistics since the level of Cerenkov light which is transmitted to the phototube is cut by the absorption of blue light in the Pb glass. In addition, Pb glasses are susceptible to yellowing by radiation. These facts make it attractive to consider a new scintillation glass, SCG1-C, recently developed by Ohara as an option for the central part of the detector (Regions I & II) and for the live converter. Beam tests done by two separate experimental groups[52-54] indicate that the energy resolutions achievable with this glass lie between $\sigma \sim 1.2\%/\sqrt{E}$ and $\sigma \sim 2.5\%/\sqrt{E}$ because of the much higher level of light available from the shower. This is to be compared to an energy resolution for SF5 which is 2-3 times worse.[55,56] One of

the groups [5] has determined this scintillation glass to be two orders of magnitude less susceptible to radiation damage. We have therefore investigated the achievable mass resolutions with a pure SF5 shower array and a mixed array with the high precision scintillation glass used in the central region. We have used the average of the present test data for the SCGl-C counter energy resolution ($\sigma \sim 2.0\%/\sqrt{E}$). The χ mass resolutions which are predicted for the two configurations are $\sigma \sim 10.5$ MeV/c^2 and $\sigma \sim 7.7$ MeV/c^2 respectively. The expected separations of the χ states are shown in figure 3a,b.

Finally, we list some of the critical parameters for the two glass types:

	SCGl-C	SF5
Radiation Length	4.35 cm	2.54 cm
Index of Refraction	1.603	1.673
Speed	∿70nsec *	$\lesssim$ 20 nsec **
Composition	$SiO_2/BaO/MgO/Li_2O/K_2O/Ce_2O_3$	$SiO_2/PbO/K_2O/Na_2O$
Density	3.41gm/cm^3	4.08gm/cm^3

*Fluorescent lifetime
**Limited by phototube signal widths

APPENDIX B

Cerenkov Counters for Charged Particle Identification

We propose to add three segmented Cerenkov counters C1, C2, and C3 to the E-537 spectrometer as indicated in Figure 1. The elevation and plan views are shown below.

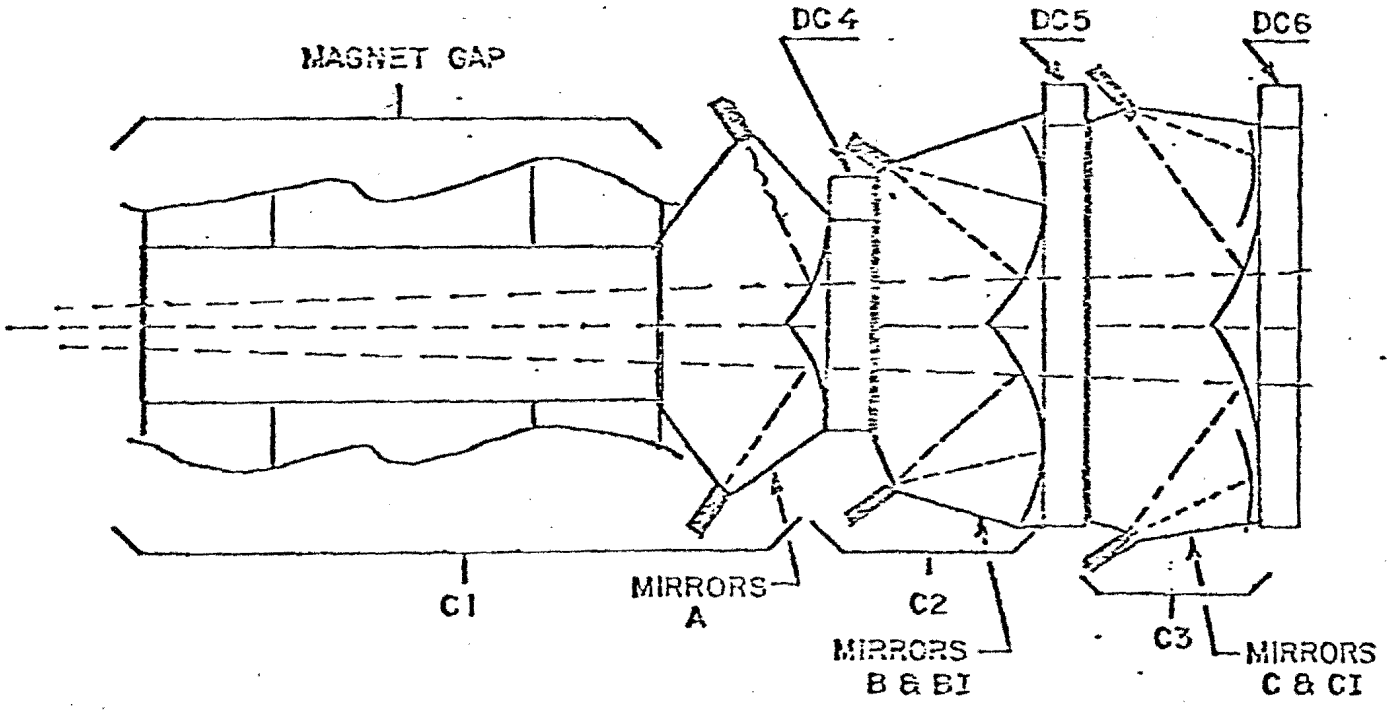

ELEVATION

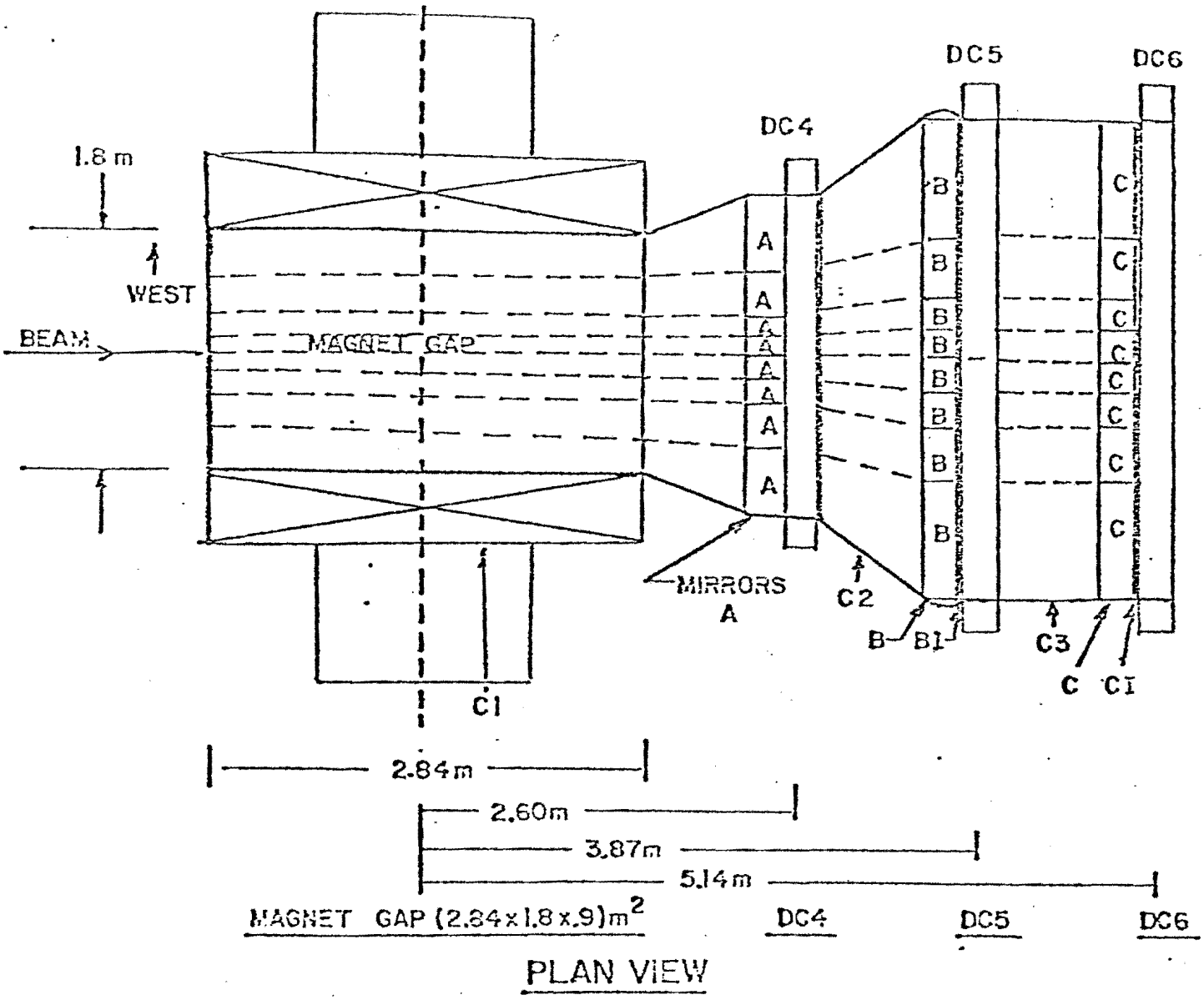

PLAN VIEW

The three Cerenkov counters have 16 cells each and cover the entire solid angle. The cell sizes have been adjusted so that the rate has been equalized in each cell. The mirrors are made out of 2mm aluminized plexiglass reinforced with honeycomb material[57] which contributes less than .005 of a radiation length. The total amount of material contributed by the three Cerenkov counters should be less than .04 of a radiation length. This is to be compared to the average radiation length of D_2 (.065RL) that the photons pass through.

The parameters of each individual counter are given in Table B1.

Table B1

Cerenkov Parameters

	C1	C2	C3
Gas	Ne(He)	Nitrogen	Freon
Refractive Index	1.000063	1.000287	1.000727
Integrated Photons/m (2200-5500A°)	15	71	180
Threshold (GeV/c) π	17	5.6	3.2
Threshold (GeV/c) K	59	20	11
Threshold (GeV/c) p	112	38	22
Average number of photo-electrons 0.5 GeV/c above threshold* π	6	8	22
Average number of photo-electrons 0.5 GeV/c above threshold* K	5	7	18
Average number of photo-electrons 0.5 GeV/c above threshold* p	5	7	18
Length (Meters)	4	1.2	1.2
Radiation Length (gas+mirrow+wall)	0.01	0.006	0.02

*These numbers were calculated assuming a photon collection efficiency of 80% and a photocathode quantum efficiency of 20%.

REFERENCES

1. E-537 Proposal, Nov. 1977, Jan. 1978/Approval letter from E. Goldwasser April 1978./P669 Proposal Submitted Jan. 1981.
2. P. Kostarakis et al., Topical Conference on the Application of Microprocessors to High Energy Physics Experiments, CERN, 4 May 81.
3. C. E. Carlson and R. Suoya, Phys. Rev. 180, (1978) 760.
4. M. Glück, J. F. Owens, and E. Reya, Phys. Rev. 17D, (1978) 2324.
5. S. D. Ellis, M. B. Einhorn, and C. Quigg, Phys. Rev. Lett. 36, (1976) 1263.
6. M. Glück and E. Reya, Phys. Lett 79B (1978) 453.
7. V. Barger, W. Y. Keung and R. J. N. Phillips, Zeitschrift für Physik C, 6, (1980) 169.
8. J. H. Kühn, Phys. Lett. 89B, (1980) 385.
9. Y. Afek, C. Leroy and B. Margolis, Phys. Rev 22D, (1980) 86.
10. R. McElhaney and S. F. Tuan, Phys. Rev D8, (1973) 2267.
11. V. Barger and R. J. N. Phillips, Nucl. Phys. B73, (1974) 269.
12. B. L. Joffe, Phys. Rev. Lett. 39 (1977) 1589.
13. E. N. Argyres and C. S. Lam, Phys. Rev. 21D (1980) 143.
14. R. M. Baltrusaitis et al., Physics Lett. 88B, (1979) 372.
15. M. Diakonou et al., Physics Lett. 87B, (1979) 292.
16. E. Amaldi et al., Physics Lett. 84B (1978) 240.
17. A. Angelis et al., Physics Lett. 94B (1980) 106.
18. L. Cormell and J. F. Owens, contributed paper, XXth International Conference, Madison, Wisconsin (1980).
19. A. P. Contogouris, S. Papdapoulos, and C. Papavassiliou, Preprint McGill University invited paper XXth International Conference, Madison, Wisconsin (1980).
20. F. Halzen and D. Scott, invited paper, XXth International Conference, Madison, Wisconsin (1980)., University of Wisconsin preprint DOE-ER/00881-15.
21. K. Kata and H. Yamamoto, preprint, University of Tokyo, UT-335 Jan. (1980).

22. R. Ruckl, S. J. Brodsky, J. F. Gunion, Physical Rev., D18 (1978) 2469.

23. Negative beam yields have been measured by the E-537 experiments at 400 GeV/c and are approximately as expected for the Λ^o and charged beams. The 1000 GeV/c yields are predicted from these measurements. The expected positive yields are estimated from the ratio of positive to negative particle yields extracted from W. F. Baker et al., Fermilab-78/79-Exp 71100.104, (1978) and W. F. Baker et al., M1 Beam Design Report.

24. B. Cox, Fermilab Report 79/1, 0090.01, January (1979).

25. B. Cox et al., P-West High Intensity Secondary Beam Area Design Report March (1977).

26. D. DeCamp et al., E.P.S. Meeting Proceedings, CERN (1979).

27. J. Badier et al., CERN/EP 79-61 (1979).

28. J. Badier et al., CERN/EP 80-149 (1980).

29. For a summary of ψ production see L. Lyons, "Massive Lepton Pair Production in Hadronic Interactions and the Quark Model", preprint-to be published in 'Progress in Particle and Nuclear Physics'.

30. T. B. W Kirk et al., Phy. Rev. Lett. 42 (1979) 619.

31. Y. Lemoigne, Proceedings of the 1979 International Symposium on Lepton and Photon Interactions at High Energies (1979) 524.

32. Y. Lemoigne et al., XX International Conference on High Energy Physics, Madison, Wisconsin (1980).

33. Particle Data Group, Reviews of Modern Physics, Vol. 52, (1980).

34. We have used the 100 GeV/c $\bar{p}p$ data of Fermilab experiment E311 for this simulation of backgrounds.

35. F. Halzen and D. Scott, Physical Rev., D18 (1978) 3778.

36. J. F. Owens and E. Reya, Phys. Rev., D17 (1978) 3003.

37. R. P. Feynman, R. D. Field, G. C. Fox, Phys. Rev., D18 (1978) 3320.

38. J. F. Owens, A. P. Contagouris, private communication.

39. G. Altarelli, G. Parisi, R. Petronzio, Phys. Lett. 76B (1978) 356.

40. See for example R. D. Field, Cal Tech Preprint CALT-68-739 for a discussion of the application of the Altarelli-Parisi method.

41. D. C. Hom et al., Phys. Rev. Lett. 36 (1976) 1239, and 37 (1976) 1374.

42. S. Witterb et al., Phys. Rev. Lett. 39 (1977) 252.

43. W. R. Innes et al., Phys. Rev. Lett. 39 (1977) 1240.

44. R. M. Baltrusaitis et al., Phys. Rev. Lett., 44 (1980) 122.

45. G. Donaldson et al., Phys. Rev. Lett. 40 (1978) 684.

46. C. Kourkoumelis et al., Phys. Lett., 84B (1979) 271, ibid 84B (1979) 277 M. Diakonou et al., Phys. Lett. 89B, (1980), C. Kourkoumelis et al., Phys. Letters 81B (1979) 405.

47. Heller et al., Nuclear Instruments and Methods 152 (1978) 379.

48. P. Garbincius et al., IEEE T-NS 27 (1980) 79.

49. Y. Bushnin et al., Nuclear Instruments and Methods 120 (1974) 391.

50. M. Atac et al., Fermilab TM-1010, (1980).

51. M. Atac et al., Fermilab CDF note, Aug. 1981 (to appear in IEEE Proceedings, Oct. 81).

52. M. Kobayashi et al., KEK Preprint 80-14, (1980).

53. S. Bartalucci et al., Frascati Preprint LNF-80/10(P) (1980).

54. M. Kobayashi et al., KEK Preprint 81-8 (1981).

55. J. A. Appel et al., Nuclear Instr. and Methods 127 (1975) 49.

56. J. E. Brau, SLAC Pub 2773, (1981) [for the Pb glass wall].

57. H. Burkhardt et al., Preprint DESY 80/10 (1980).

58. R. Barate et al., XX International Conference on High Energy Physics, Madison, Wisconsin (1980).

59. H. Fritzsch, Workshop on New Flavors, College de France (1979) Physics Lett. 86B (1979) 343.

E-537/P-669
SPECTROMETER

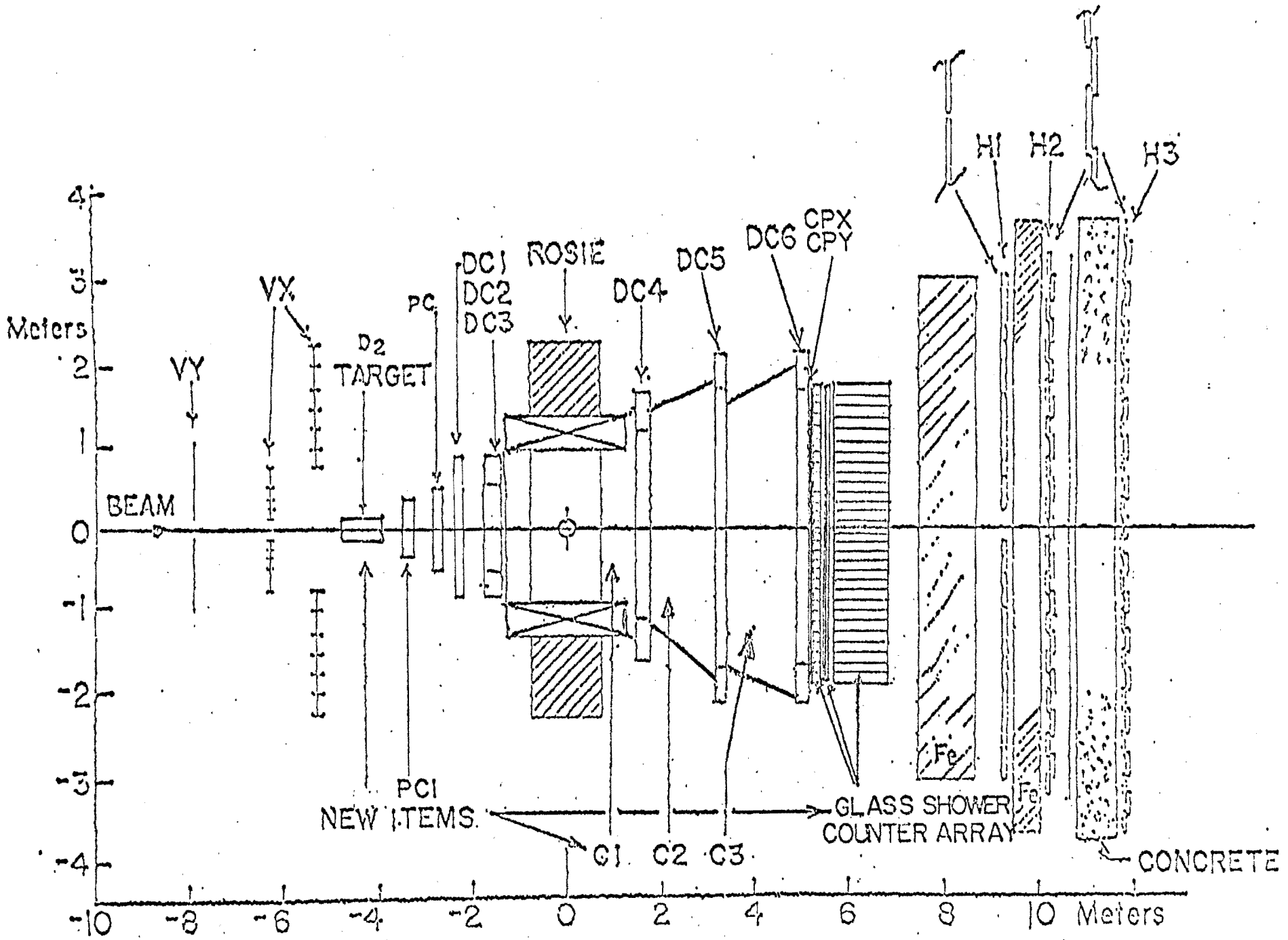

FIGURE 1

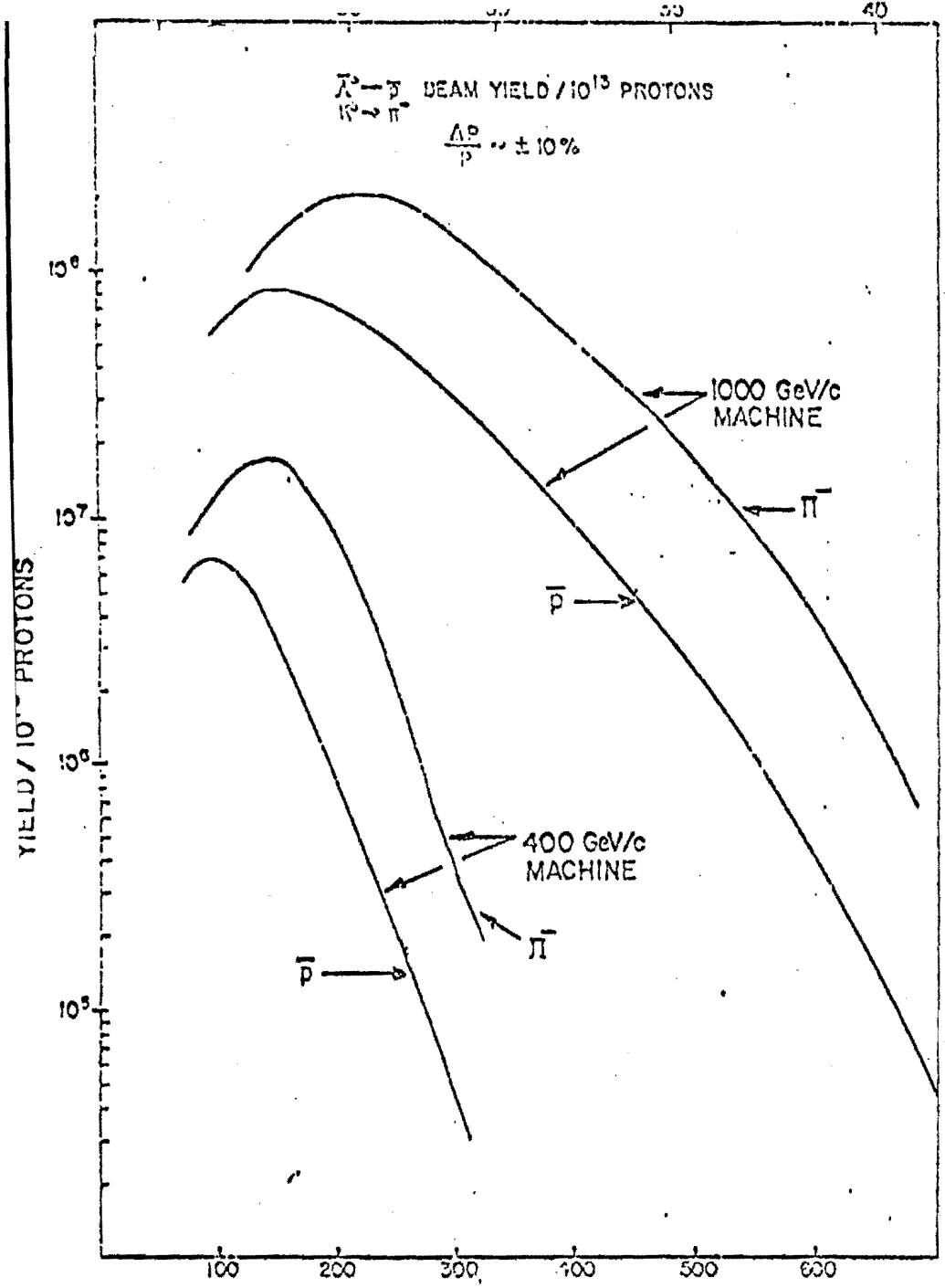

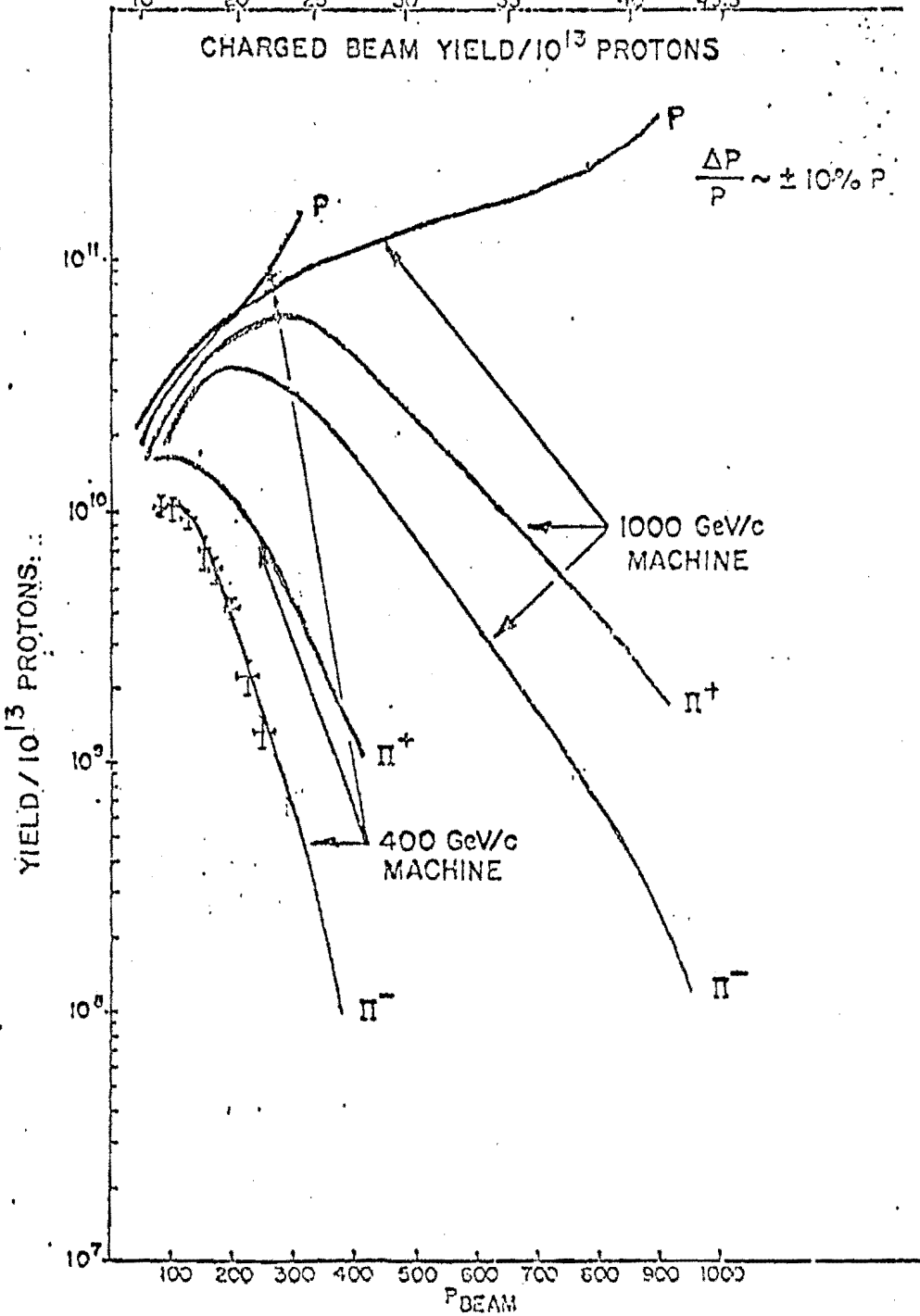

FIGURE 2
HIGH INTENSITY LABORATORY
YIELD CURVES

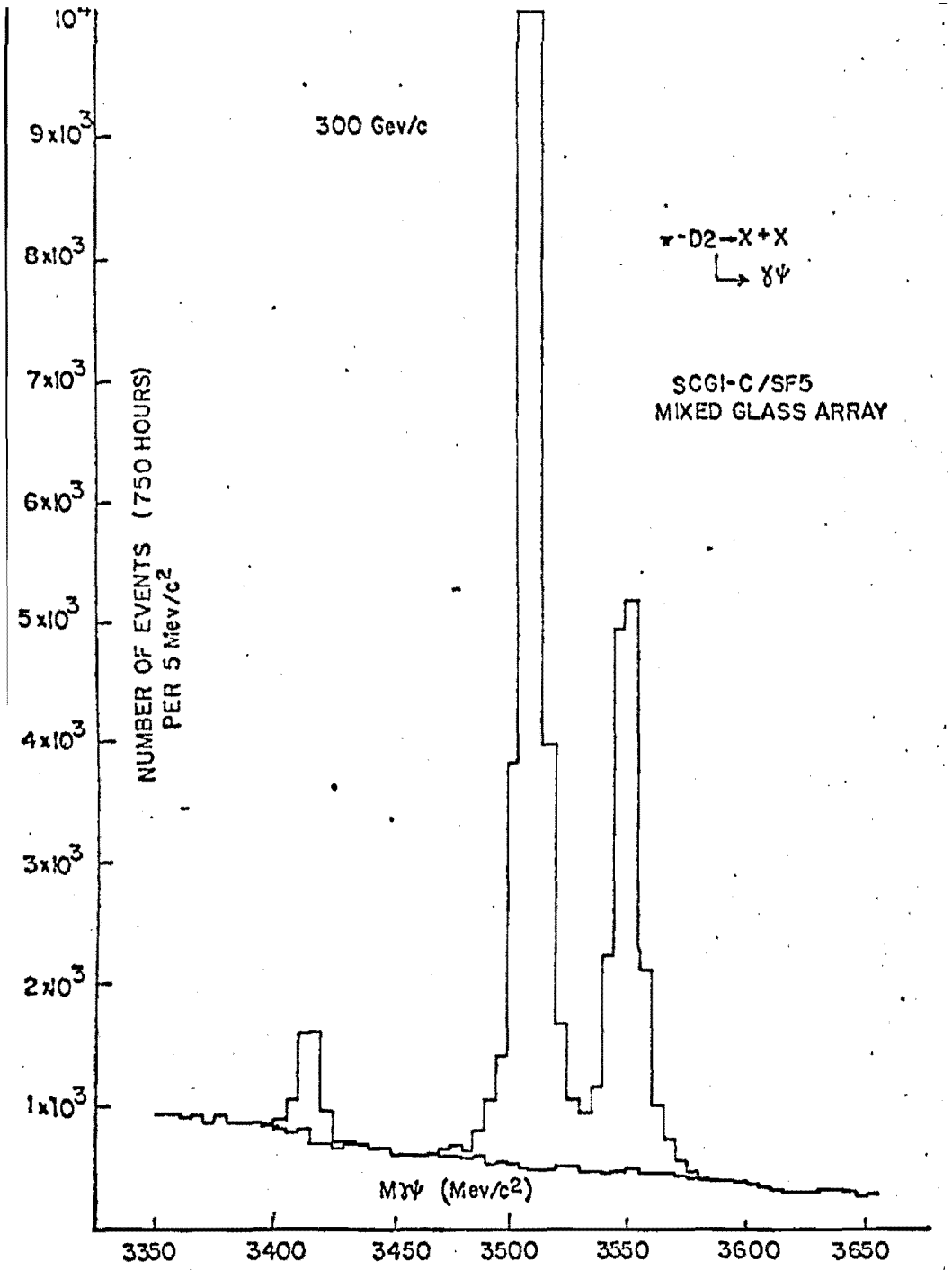

Figure 3a

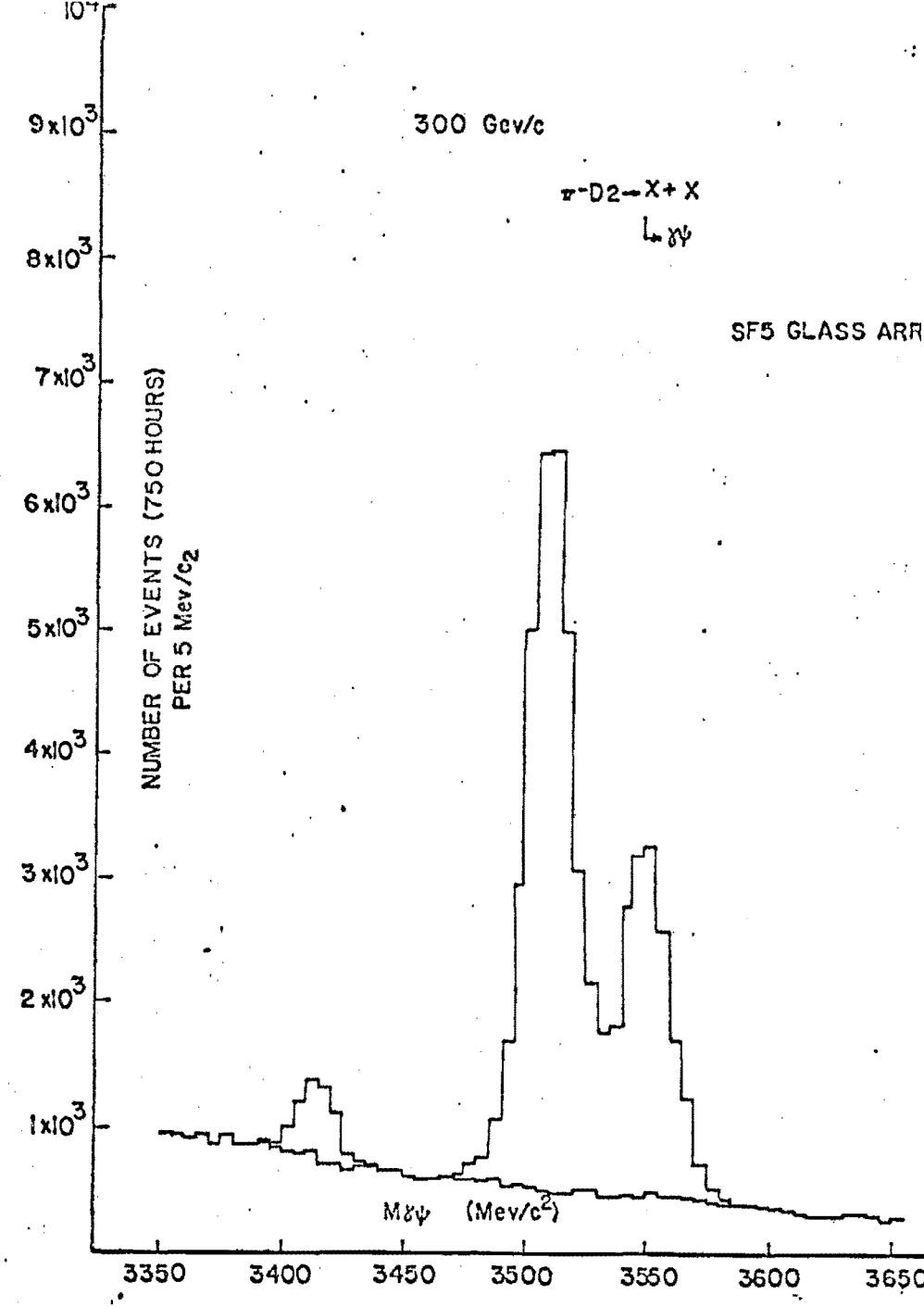

Figure 3b

Position resolution:

$\frac{\sigma}{\sqrt{E}} \sim \frac{11}{\sqrt{E}}$ mm Refs 47, 48, 49, 50, 51

Energy resolution-Mixed Glass Composition

Inner Detector $\frac{\sigma}{\sqrt{E}} \sim \frac{2\%}{\sqrt{E}}$ Refs 52, 53. 54

Outer Detector $\frac{\sigma}{\sqrt{E}} \sim \frac{4.3\%}{\sqrt{E}}$ + .7 % Refs.55,56

Energy resolution SF5 Glass Composition

$\frac{\sigma}{\sqrt{E}} \sim \frac{4.3\%}{\sqrt{E}}$ + .7 % Refs.55,56

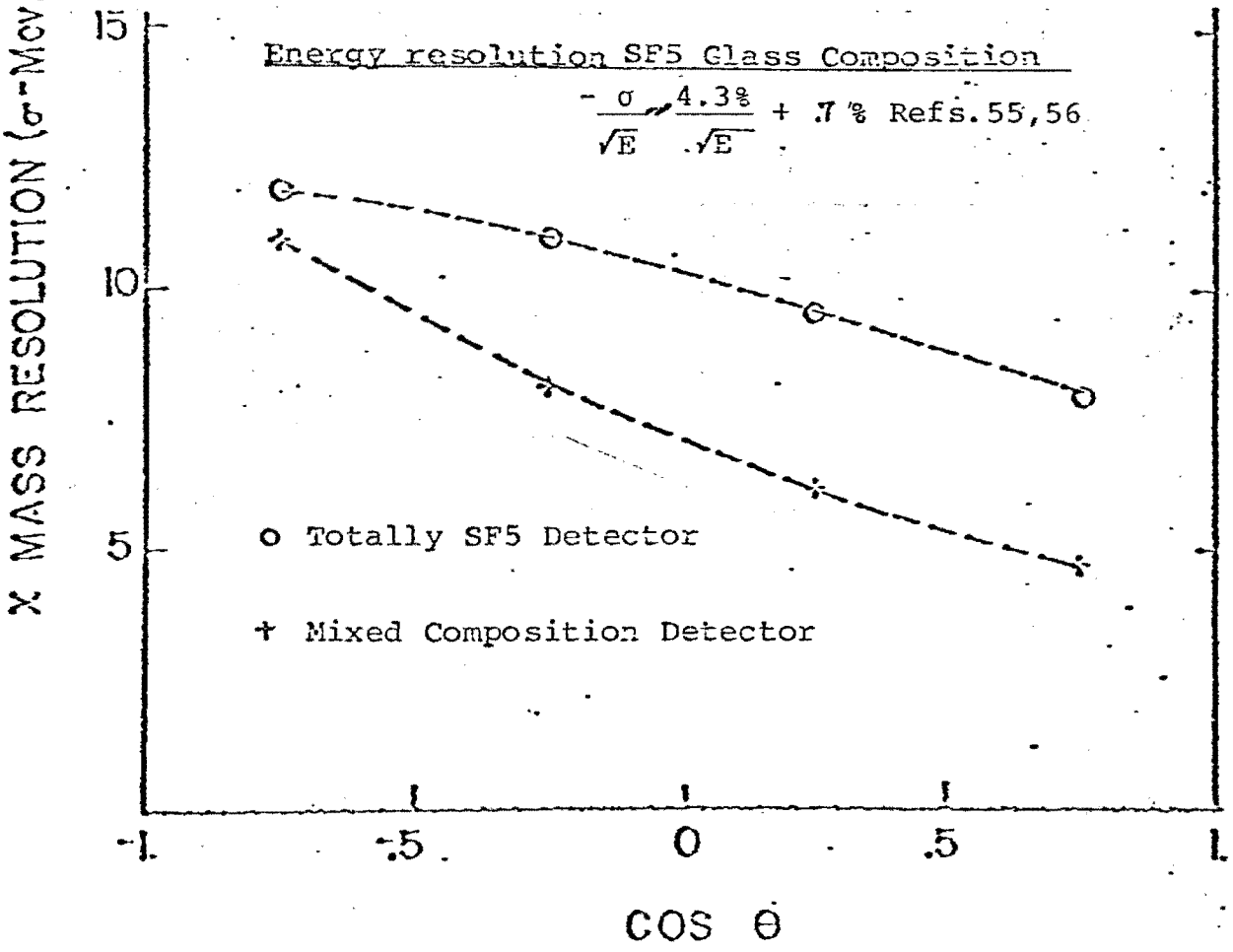

θ : Angle between photon and beam in the χcms

Figure 4

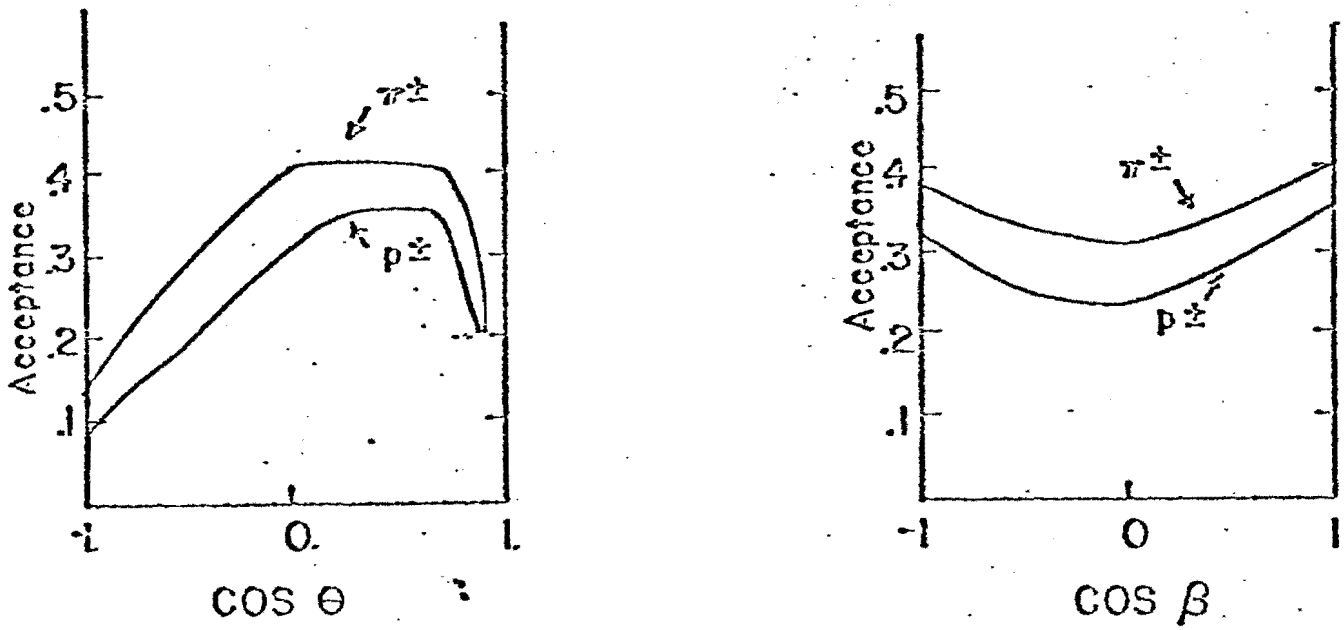

θ : between photon and beam in the χcm

β : between photon and lepton in the χcm

Figure 5

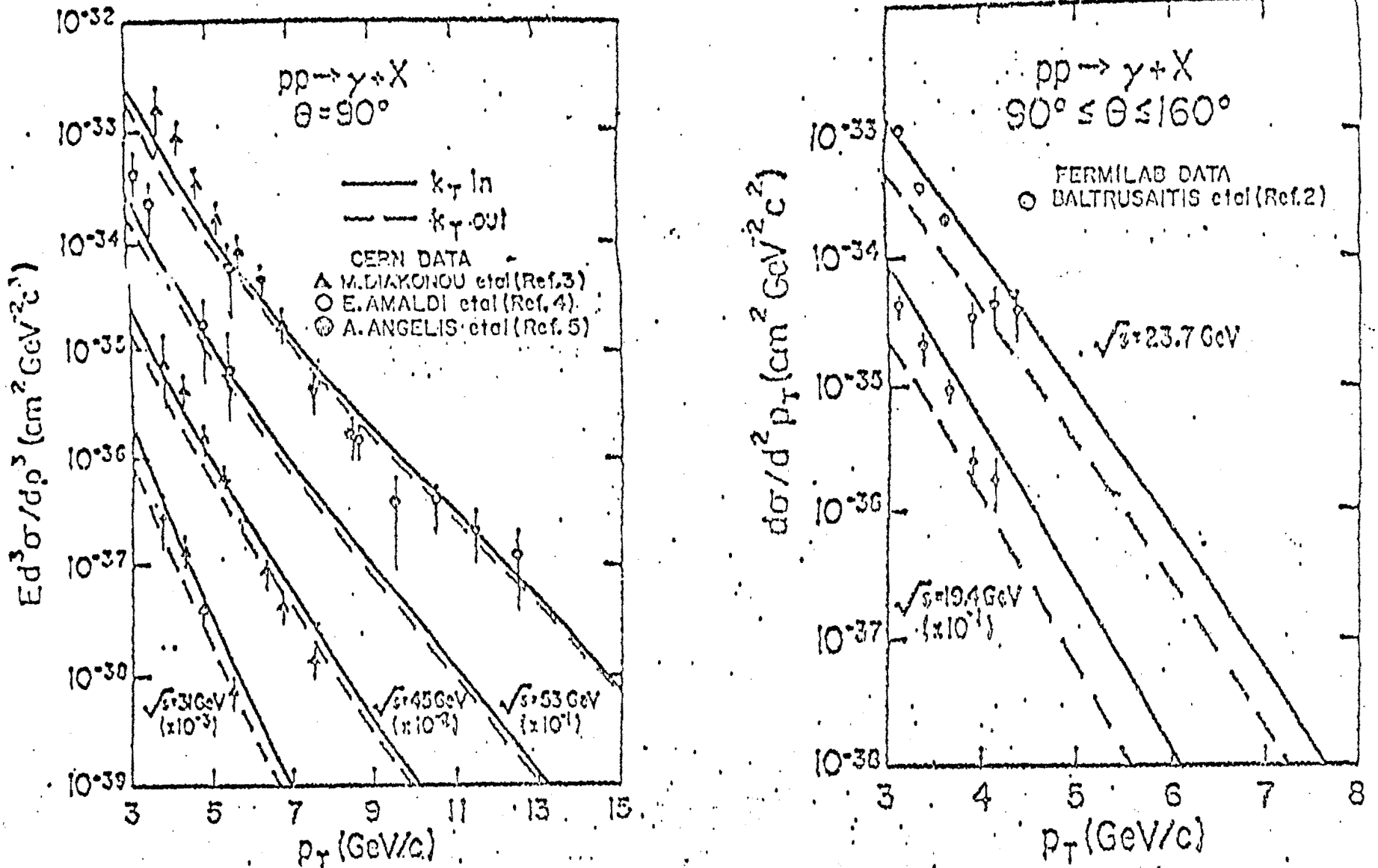

FIGURE 6

EXISTING pp → γX DATA

FIGURE 7a

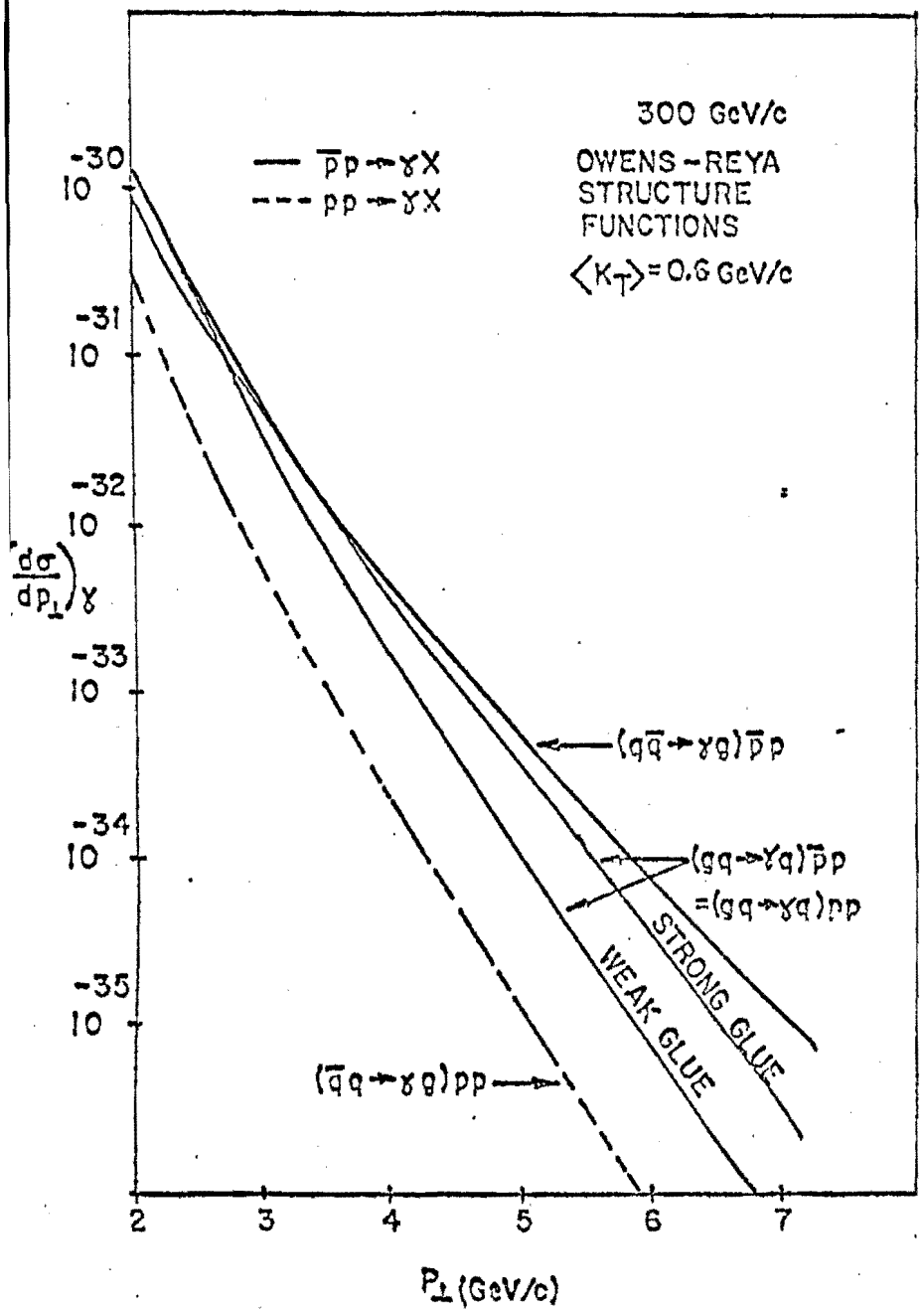

FIGURE 7b

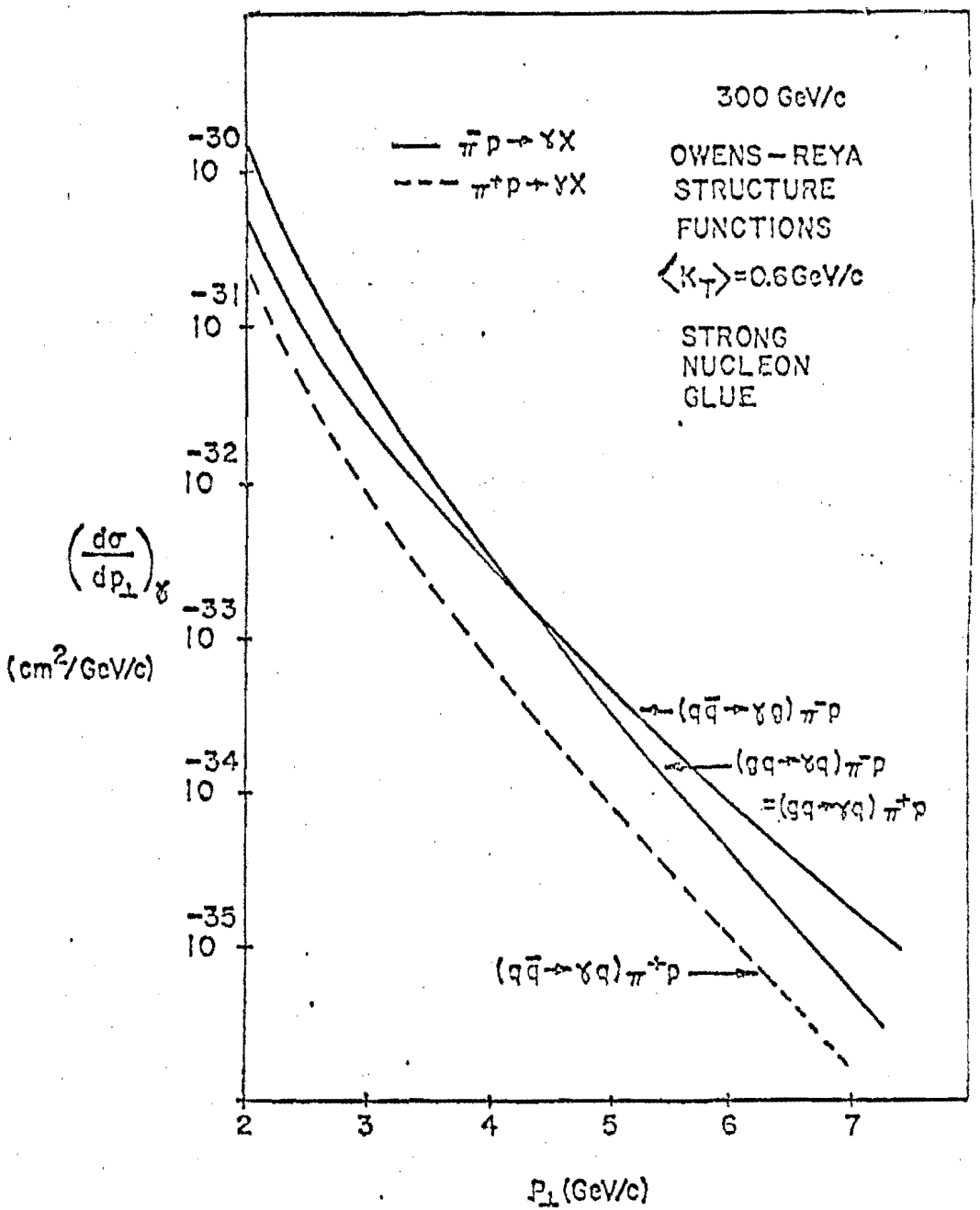

CROSS SECTIONS Vs $P_\perp$ FOR DIRECT PHOTON PROCESS

FIGURE 8a

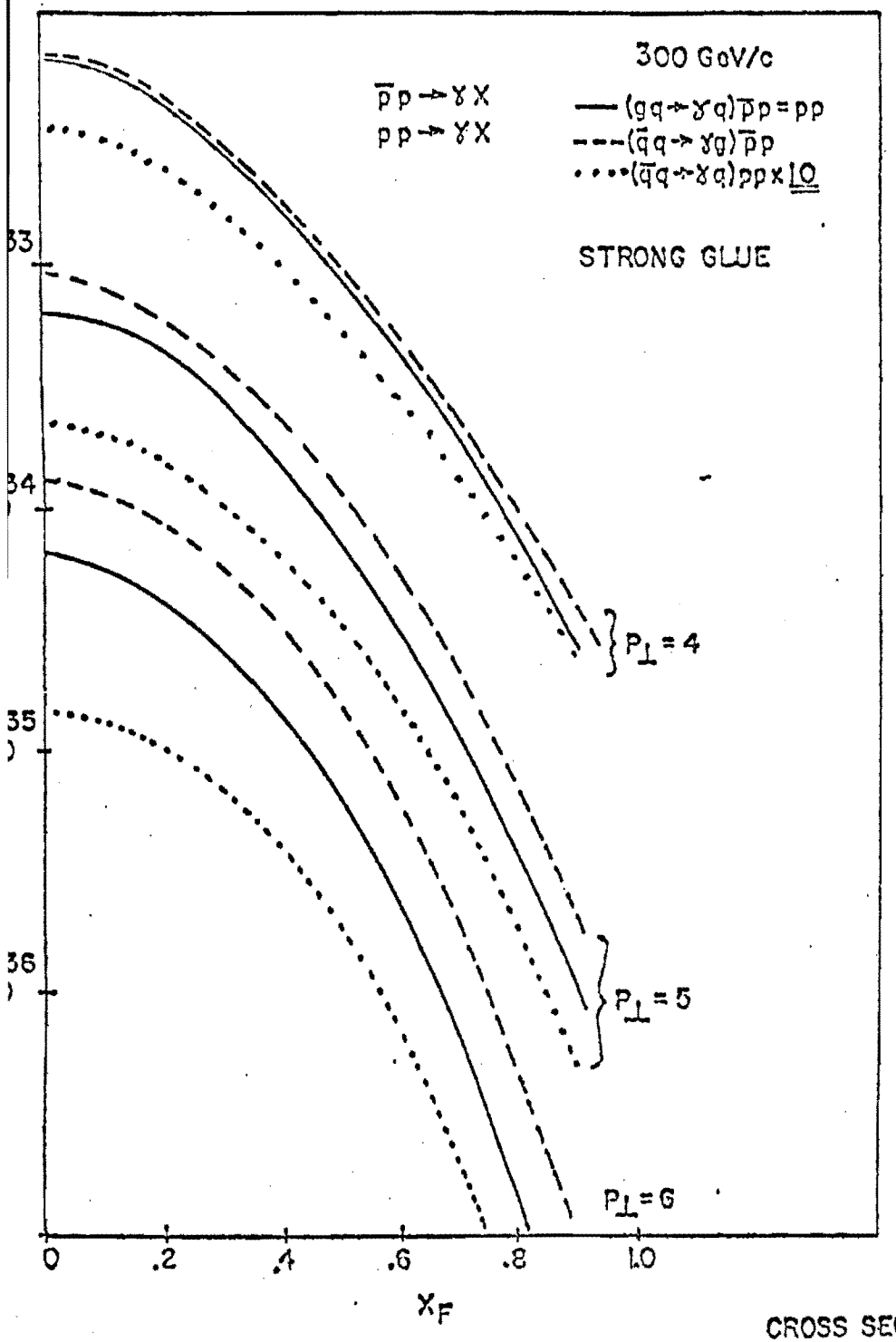

FIGURE 8b

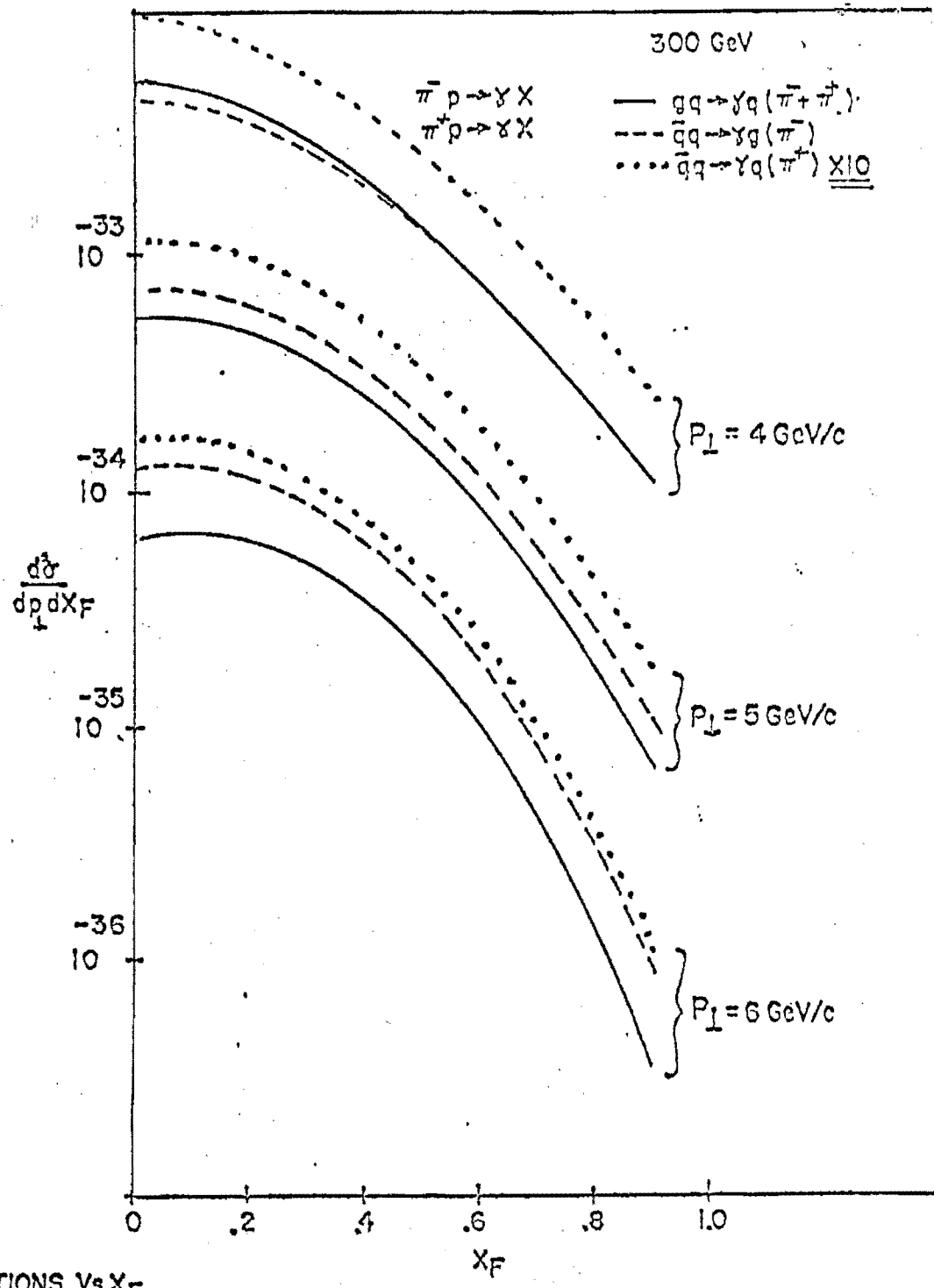

CROSS SECTIONS Vs X_F
FOR THE DIRECT PHOTON
PROCESS

Figure 9a

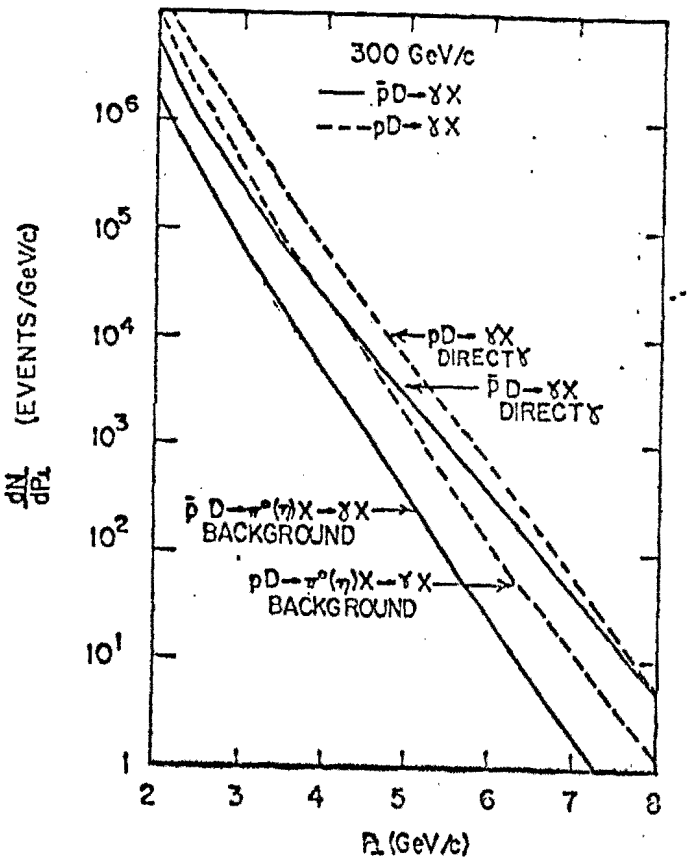

Figure 9b

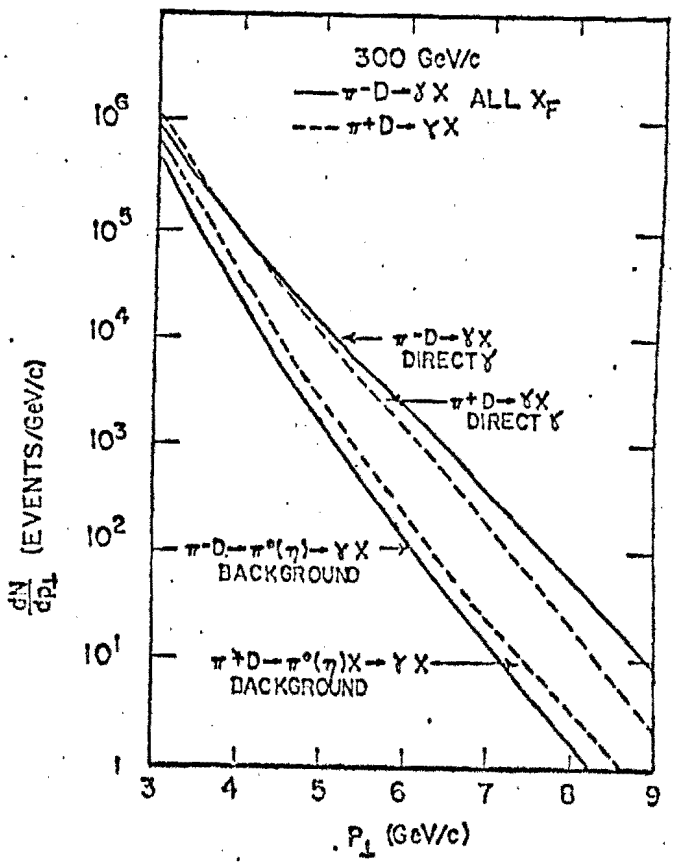

Number of Direct Photon and Background Events

Vs. $P_\perp$ (750 Hours Run)

Figure 10a

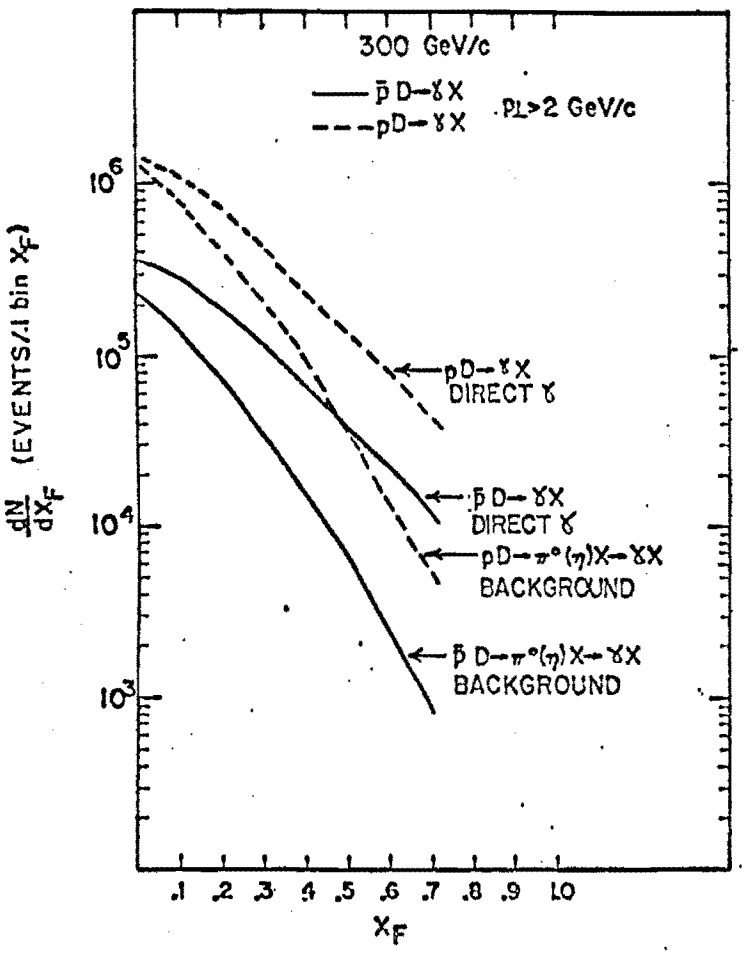

Figure 10b

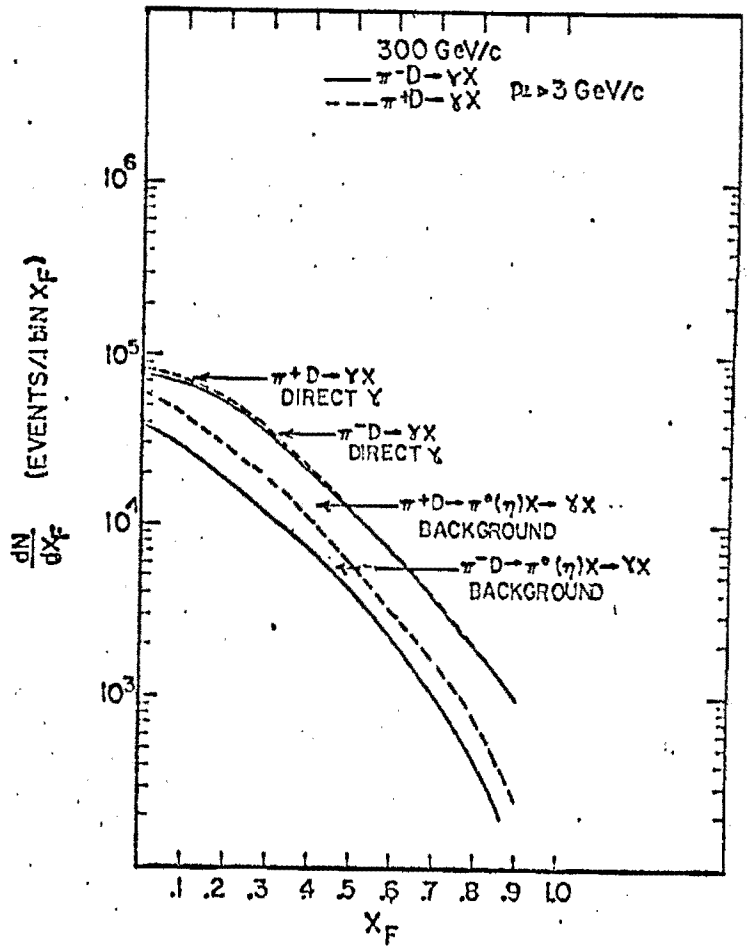

Number of direct photon and background events vs. X_F

(750 hours run)